J Supercond Nov Magn (2016) 29:3023–3026
DOI 10.1007/s10948-016-3848-9

ORIGINAL PAPER

Two-Dimensional Nanogranularity of the Oxygen Chains in the $YBa_2Cu_3O_{6.33}$ Superconductor

G. Campi[1] · A. Ricci[2] · N. Poccia[3,4] · A. Bianconi[1,3]

Received: 6 October 2016 / Accepted: 8 October 2016 / Published online: 18 October 2016

Abstract The organization of dopants in high-temperature superconductors provides complex topological geometries that control superconducting properties. This makes the study of dopants' spatial distribution of fundamental importance. The mobile oxygen ions, y, in the CuO_2 plane of $YBa_2Cu_3O_{6+y}$ ($0.33 < y < 0.67$) form ordered chains which greatly affect the transport properties of the material. Here, we visualize and characterize the two-dimensional spatial organization of these oxygen chains using scanning micro X-ray diffraction measurements in transmission mode on a thin single-crystal slab with $y = 0.33$ ($T_c = 7$ K) near the critical doping for the insulator-to-metal transition. We show the typical landscape of percolation made of a granular spatial pattern due the oxygen chains segregating in quasi-one-dimensional needles of ortho-II (O-II) phase embedded in an insulating matrix with low density of disordered oxygen interstitials.

Keywords Micro X ray diffraction · Spatial statistics · Superconductivity

✉ G. Campi
gaetano.campi@ic.cnr.it

[1] Institute of Crystallography, CNR, Via Salaria Km 29.300, Monterotondo, 00015 Rome, Italy

[2] Deutsches Elektronen-Synchrotron (DESY), Notkestraße 85, 22607 Hamburg, Germany

[3] Rome International Center for Materials Science Superstripes (RICMASS), Via dei Sabelli 119A, 00185 Rome, Italy

[4] MESA+ Institute for Nanotechnology, University of Twente, PO Box 217, 7500 AE Enschede, The Netherlands

New and complex functional materials are characterized by structural heterogeneity giving rise to textures and granular patterns at different scale lengths. The emergence of multiscale patterns, from the microscale down to the nanoscale, gives new physical-chemical properties in several classes of materials belonging to different research fields such as chemistry [1, 2], material engineering [3], and biomedicine [4–6], just to mention a few.

High-temperature superconductors constitute an intriguing class of materials where the separation and competition of multiple phases at nanoscopic scale occurs [7–11]. These inhomogeneous phases are due to the ordering of dopants and competition between short-range charge-density wave (CDW), spin-density wave (SDW), and orbital density wave (ODW) order inhomogeneity. As a result, new complex geometries emerge, where quantum coherence develops [12–14]. Thus, the study of local features by using high-resolution experimental probes assumes a paramount importance for a deeper understanding of new complex and heterogeneous materials. Local probes such as X-ray absorption experimental methods (XANES and EXAFS) and high-resolution X-ray and neutron diffraction have been used for investigating the structural inhomogeneity in various systems such as diborides [15–17] and cuprates [18–20]. In the last years, the possibility to focus an X-ray beam onto micrometric and sub-micrometric areas has allowed to probe the local structure with high resolution in the real space. More specifically, for example, microbeams have been used for mapping weak diffuse scattering in the real space in scanning micro X-ray diffraction (SμXRD) measurements. The collected data, treated by spatial statistical tools, have shown the formation of fractal patterns of interstitial oxygen-ordered domains in LCO [21], intrinsic phase separation in doped iron chalcogenides

[22, 23], and planar symmetry breaking in bismuthates [24]. More recently, it has been demonstrated that the quenched disorder due to dopants is spatially anti-correlated with electronic textures and/or local lattice distortions in Hg1201 [12, 13] and LCO [25]. Thus, the oxygen-striped domains are a candidate to provide the space where superconductivity arises. This makes the study of quenched disorder and its spatial distribution of fundamental importance.

$YBa_2Cu_3O_{6+y}$ (YBCO) is one of the most studied high-temperature superconductors due to its simple synthesis route and because it was the first superconductor to be discovered with T_c above the liquid nitrogen temperature. Here, oxygen dopants get ordered in Cu–O chains that attract electrons from the CuO_2 layers. This ordering gives rise to "guest superstructures" detected as satellite peaks in diffraction patterns [26–30]. The spatial distribution of different superstructures has been investigated by us using X-ray diffraction in reflection mode, probing the vertical plane ac [27, 30].

In this work, we employed micro X-ray diffraction in transmission mode on a thin slab of $YB_2C_3O_{6.33}$ with the tetragonal-orthorhombic phase boundary, for visualizing the oxygen chain arrangement on the basal CuO_2 planes. At this oxygen concentration, superconductivity coexists with the anti-ferromagnetism, although both are strongly suppressed. The $YBa_2Cu_3O_{6.33}$ single crystals were grown in yttrium-stabilized zirconia crucibles by a flux growth method using chemicals of 99.999 % purity for Y_2O_3 and CuO and of 99.997 % for $BaCO_3$. The impurity level of the crystals has been analyzed by inductively coupled plasma mass spectroscopy. The Zr content of the crystals was found to be less than 10 ppm by weight. The major impurities were Al, Fe, and Zn, the sum of which amounts to less than 0.2 % atom per unit cell. The oxygen composition of the crystals was changed by the use of gas volumetric equipment. The technique allows to determine the oxygen composition with an accuracy better than $\Delta x = 0.02$. The superconducting critical temperature is found to be $T_c = 7$ K.

Standard X-ray diffraction measurements were performed at an XRD beamline of ELETTRA in Trieste, Italy [31], using a photon energy of 20 keV and a Mar Research 165-mm charge-coupled device (CCD) camera. The unit cell of $YBa_2Cu_3O_{6.33}$ single crystal has $a = 3.851(4)$ Å and $c = 11.78(5)$ Å, in the I4mm space group. We found superlattice reflections associated to the ortho-II phase, located at positions $\mathbf{q_{O-II}} = (h \pm 1/2, k \pm 1/2, l)$ with h, k, and l as integers. In Fig. 1a, b, we show the diffraction profiles along a^* and b^* directions, respectively, of the $(-2.5, 0, 0)$ streak satellite reflection, measured at the XRD beamline of ELETTRA, fitted by Gaussian line profiles. A pictorial view of the phase separation due to the arrangement of oxygen ions in linear chains with periodicity of two unit cells along a and b directions is shown in Fig. 1c. The Oi-rich domains (with Oi chain fragments) form nanoscale O-II phase coexisting with domains with poor and disordered oxygen.

The spatial distribution of these Oi-rich domains has been studied by SμXRD measurements in transmission mode performed at the ID13 beamline of the European Synchrotron Radiation Facility (ESRF), Grenoble, France. We used a monochromatic X-ray beam with an energy of 14 keV ($\Delta E/E = 10^{-4}$) focused by Kirkpatrick–Baez (KB) mirrors to a 1-μm spot size on the sample. A 16-bit two-dimensional fast readout low noise charged coupled device (FReLoN CCD) detector with 2048 × 2048 pixels of 51 × 51 μm^2 was used, binned to 512 × 512 pixels. Diffraction images were obtained after correcting the two-dimensional images for dark-noise, flat-field, spatial distortion. This satellite

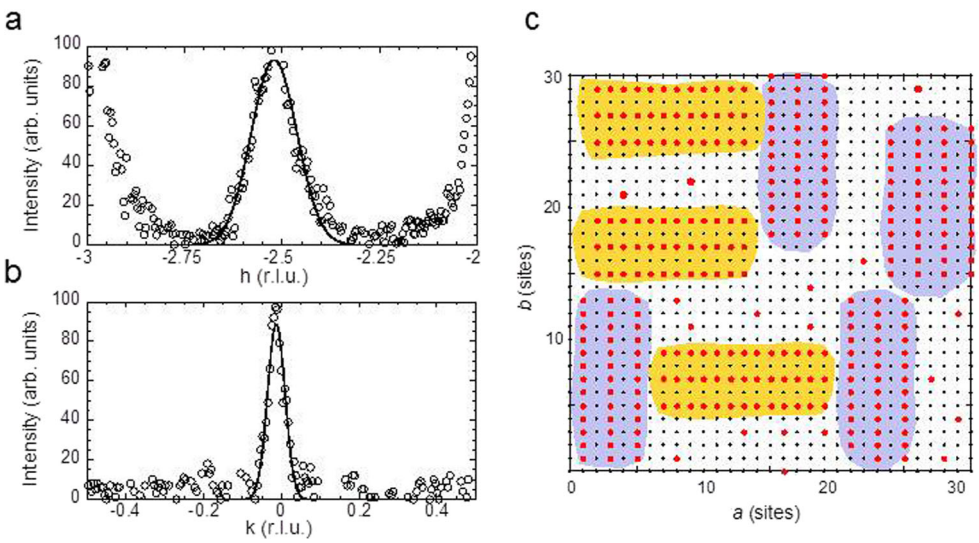

Fig. 1 *Open circles* X-ray diffraction profile of the O-II superlattice with wavevector $\mathbf{q_{O-II}} = -2.5$ h, along a^* (**a**) and b^* (**b**) directions. *Continuous lines* indicate the Gaussian fits. **c** Oxygen defect Oi (*red full circles*) and Cu (*black dots*) sites forming the basal CuO_2 planes. The ortho-II phase (*shadowed areas*) made of horizontal and vertical Oi chains is embedded in domains with disordered poor oxygen

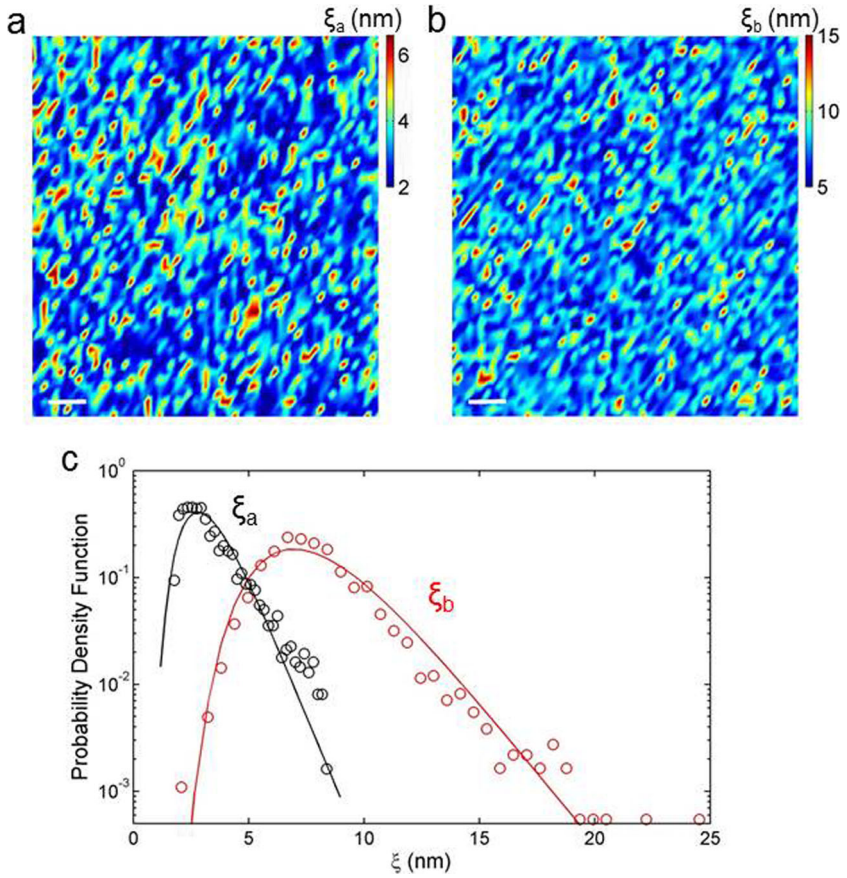

Fig. 2 Color map of the O-II correlation length along the *a* (**a**) and *b* (**b**) directions. The O-II superstructure in plane size domains is plotted as a function of the illuminated spot position along the *a* and *b* crystallographic axis of the sample. The *white bar* indicates a 25-μm-length scale on the sample surface. **c** Semi-log plot of spatial distribution of domain size along *a-axis* and *b-axis* of O-II superlattices. We have used a lognormal function (*continuous lines*) to model the probability density functions

reflection was then measured at each point of the sample reached by the x–y translator with sub-micron resolution in order to visualize the point-to-point spatial variation of both intensity and size of the *ortho-II* domains. The correlation lengths along the a and b directions, ξ_a and ξ_b, of the ortho-II domains, have been derived from the measured FWHM via standard methods of diffraction. The spatial distributions of ξ_a and ξ_b are shown by the maps in Fig. 2a,b, respectively. We can clearly observe the inhomogeneous character of the size of the ordered domains. In order to characterize this spatial texture, we calculated the probability density function of both ξ_a and ξ_b (see Fig. 2c). As previously determined by the statistical analysis of domain sizes, some deviations from normal behavior are observed in the right tails of distribution [27–30]. These deviations can be quantified by the distribution skewness (sk), giving $\mathrm{sk}_a = 1.35$ and $\mathrm{sk}_b = 28.5$ for the ortho-II domain size along the a and b directions, respectively. Indeed, the probability density function of ξ, as shown in Fig. 2c, appears clearly with a fatter tail in the (long) b direction. The correlation lengths range from 2 to 8 nm in the (short) a direction and from 4 to 30 nm in the (long) b direction. It is well known how deviations from a normal distribution in the right tail of a distribution are related with a more complex behavior in several systems and processes [32]. In this case, the fatter tails suggest a complex morphology for the granular *ab* surface due to the presence of *few* large domains coexisting with *many* small domains of Oi chains.

This is confirmed by investigating the interplay between the density and size of Oi-rich chain domains by the scatter plot of the domain size along a and b as a function of $\mathbf{q_{O-II}}$ superstructure intensity (Fig. 3). We note that the size of ordered domains along b is anti-correlated with the domain

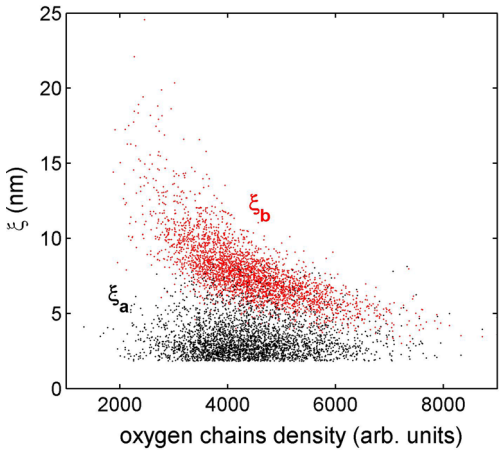

Fig. 3 Scatter plot of correlation lengths ξ_a and ξ_b as a function of streak intensity giving the density of Oi chains

population; in other words, we have few large domains and many small domains along b. On the other side, we get a quit random relationship between the domain population and domain size along a.

In summary, we have studied the planar granularity due to the oxygen order in $YBa_2Cu_3O_{6.33}$. We measured the local variations of oxygen ordered domains by analyzing the satellite reflections associated to the ortho-II needle-like domains made of oxygen chains running along the a and b directions. Our observations clearly show that chains ordering in YBCO produce a phase separation between two-dimensional ordered and disordered domains with poor oxygen content ($y < 0.33$) with the typical complex topology of a superstripe landscape [33]. The ordered O-II domains form quasi-one-dimensional needles with a distribution of size ranging between 2 and 8 nm in the transversal direction and between 3 and 30 nm along the needle direction. Finally, we would remark that our XRD experiment shows that $YBa_2Cu_3O_{6.33}$ is made of $YBa_2Cu_3O_6$ with a percolating concentration of 66 % of $YBa_2Cu_3O_{6.5}$ needles. Therefore, it is possible that the spatial topology for the emergence of high-temperature superconductivity is given by the interface space between the one-dimensional O-II needles with can give a hyperbolic space [12, 13].

References

1. Campi, G., Mari, A., Pifferi, A., Amenitsch, H., Fratini, M., Suber, L.: Nanoscale **3**, 3774–3779 (2011). doi:10.1039/C1NR10474H
2. Cannas, C., Ardu, A., Musinu, A., Suber, L., Ciasca, G., Amenitsch, H., Campi, G.: ACS Nano **9**(7), 7277–7286 (2015). doi:10.1021/acsnano.5b02145
3. Li, H., Xiao, H.G., Yuan, J., Ou, J.: Microstructure of cement mortar with nano-particles. Compos. Part. B **35**(2), 185–189 (2004)
4. Campi, G., Pezzotti, G., Fratini, M., Ricci, A., Burghammer, M., Cancedda, R., Mastrogiacomo, M., Bukreeva, I., Cedola, A.: Appl. Phys. Lett. **103**, 253703 (2013)
5. Campi, G., Fratini, M., Bukreeva, I., Ciasca, G., Burghammer, M., Brun, F., Tromba, G., Mastrogiacomo, M., Cedola, A.: Acta Biomaterialia **23**, 309–316 (2015). doi:10.1016/j.actbio.2015.05.033
6. Poccia, N., Campi, G., Ricci, A., Caporale, A.S., Di Cola, E., Hawkins, T., Bianconi, A.: Sci. Rep. **4**, 5430 (2014)
7. Dagotto, E.: Complexity in strongly correlated electronic systems. Science **309**, 257–262 (2005)
8. Campi, G., Innocenti, D., Bianconi, A.: J. Supercond. Nov. Magn. **28**(4), 1355–1363 (2015)
9. Giraldo-Gallo, P., Zhang, Y., Parra, C., et al.: Nat. Commun. **6**, 8231 (2015)
10. Zaanen, J.: Nature **466**, 825–827 (2010)
11. Chang, J., et al.: Nat. Phys. **8**, 871–876 (2012)
12. Campi, G., Bianconi, A., Poccia, N., et al.: Nature **525**, 359 (2015). doi:10.1038/nature14987
13. Campi, G., Bianconi, A.: J. Supercond. Nov. Magn. **29**, 627 (2016). doi:10.1007/s10948-015-3326-9
14. Carlson, E.W.: Nature **525**, 329–330 (2015)
15. Campi, G., Cappelluti, E., Proffen, T., Qiu, X., Bozin, E.S., Billinge, S., Agrestini, N., Saini, L., Bianconi, A.: Eur. Phys. J. B **52**, 15 (2006)
16. Campi, G., Ricci, A., Bianconi, A.: J. Supercond. Nov. Magn. **25**(5), 1319–1322 (2012)
17. Agrestini, S., Metallo, C., Filippi, M., Campi, G., Sanipoli, C., De Negri, S., Giovannini, M., Saccone, A., Latini, A., Bianconi, A.: J. Phys. Chemistry Solids **65**, 1479 (2004)
18. Saini, N.L., Oyanagi, H., Ito, T., Scagnoli, V., Filippi, M., Agrestini, S., Campi, G., Oka, K., Bianconi, A.: Eur. Phys. J. B **36**, 75 (2003)
19. Campi, G., Di Castro, D., Bianconi, G., Agrestini, S., Saini, N.L., Oyanagi, H., Bianconi, A.: Phase Transit. **75**, 927 (2002)
20. Bianconi, A., Missori, M., Oyanagi, H., Yamaguchi, H., Ha, D.H., Nishiara, Y., Della Longa, S.: Europhys. Lett. **31**, 411–415 (1995)
21. Fratini, M., Poccia, N., Ricci, A., Campi, G., Burghammer, M., Aeppli, G., Bianconi, A.: Nature **466**, 841 (2010)
22. Ricci, A., Poccia, N., Campi, G., Joseph, B., Arrighetti, G., Barba, L., Reynolds, M., Burghammer, M., Takeya, H., Mizuguchi, Y., et al.: Phys. Rev. B **84**, 060511 (2011)
23. Ricci, A., Poccia, N., Joseph, B., Innocenti, D., Campi, G., Zozulya, A., Westermeier, F., Schavkan, A., Coneri, F., Bianconi, A., Takeya, H., Mizuguchi, Y., Takano, Y., Mizokawa, T., Sprung, M., Saini, N.L.: Phys. Rev. B **91**(R), 020503 (2015)
24. Poccia, N., Campi, G., Fratini, M., Ricci, A., Saini, N.L., Bianconi, A.: Phys. Rev. B **84**, 100504 (2011)
25. Poccia, N., Ricci, A., Campi, G., Fratini, M., Puri, A., Di Gioacchino, D., Marcelli, A., Reynolds, M., Burghammer, M., Saini, N.L., Aeppli, G., Bianconi, A.: Proc. Natl. Acad. Sci. U.S.A. **109**(39), 15685–15690 (2012)
26. von Zimmermann, M., Schneider, J.R., Frello, T., Andersen, N.H., Madsen, J., Käll, M., Poulsen, H.F., Liang, R., Dosanjh, P., Hardy, W.N.: Phys. Rev. B **68**, 104515 (2003)
27. Campi, G., Ricci, A., Poccia, N., Barba, L., Arrighetti, G., Burghammer, M., Caporale, A.S., Bianconi, A.: Phys. Rev. B **87**, 014517 (2013)
28. Ricci, A., Poccia, N., Campi, G., Coneri, F., Caporale, A.S., Innocenti, D., Burghammer, M., Zimmermann, M.V., Bianconi, A.: Scientific Reports **3**, 2383 (2013)
29. Ricci, A., Poccia, N., Campi, G., Coneri, F., Barba, L., Arrighetti, G., Polentarutti, M., Burghammer, M., Sprung, M., Zimmermann, M., Bianconi, A.: New J. Phys. **16**, 053030 (2014)
30. Campi, G., Ricci, A., Poccia, N., Bianconi, A.: J. Supercond. Nov. Magn. **27**(4), 987–990 (2014)
31. Lausi, A., Polentarutti, M., Onesti, S., Plaisier, J.R., Busetto, E., Bais, G., Barba, L., Cassetta, A., Campi, G., Lamba, D., Pifferi, A., Mande, S.C., Sarma, D.D., Sharma, S.M., Paolucci, G.: Euro. Phys. J. Plus **130**(3), 1–8 (2015)
32. Altamura, M., Elvevag, B., Campi, G., De Salvia, M., Marasco, D., Ricci, A., Bellomo, A.: Complexity **18**(1), 38–43 (2012)
33. Bianconi, A.: Int. J. Mod. Phys. B **14**, 3289 (2000)